

Raman spectroscopy in heavy-mineral studies

SERGIO ANDÒ & EDUARDO GARZANTI*

*Laboratory for Provenance Studies, Università di Milano-Bicocca,
Piazza della Scienza 4, 20126 Milano, Italy*

**Corresponding author (e-mail: eduardo.garzanti@unimib.it)*

Abstract: Raman spectroscopy is an innovative tool with tremendous potential, serving as a fundamental complement to a variety of provenance methods including heavy-mineral analysis and detrital geochronology. Because of its accuracy, efficiency and versatility, the results of the Raman technique are indispensable for fully reliable identification of heavy minerals in grain mounts or thin sections. Thorny long-standing problems that cannot be solved confidently with a polarizing microscope alone, such as the determination of opaque and altered heavy minerals, of detrital grains as small as a few microns, or of colourless crystals with uncertain orientation and rounded morphology, can finally be addressed. Although the method can be highly automated, the full ability and experience of the operator is required to combine Raman data with the optical information obtained under the microscope on the same grains, which is essential for the efficient application of the method in provenance studies. This article provides exemplary Raman spectra useful for the comparison and determination of over 70 different opaque and transparent heavy-mineral species commonly found in sediments, conveying specific information on the genesis of their source rocks, and thus is particularly useful in provenance diagnoses and palaeotectonic reconstructions.

Supplementary material: Detailed information on the lasers used and the origin of the analysed minerals is available at <http://www.geolsoc.org.uk/SUP18615>

It is the scattering of light by atoms and molecules that gives us the light of the sky, the blue colour of the deep sea and the delicate opalescence of large masses of clear ice. (Raman 1928, pp. 368–369)

Raman spectroscopy is a user-friendly, efficient and innovative technique that is the ideal complementary tool to the heavy-mineral analysis carried out under a polarizing microscope. The method is non-destructive, does not require specific preparation, and can be used directly on both heavy-mineral slides and thin sections (Griffith 1969; McMillan 1989; Hope *et al.* 2001; Nasdala *et al.* 2004). It can be used to investigate the very same grains that have been counted under the optical microscope, to identify undetermined grains, including opaque or weathered turbid accessory minerals, and to facilitate the elimination of operator error. Moreover, additional information can be obtained on polymorphs, hydrated minerals, carbonaceous materials, weathering products and solid, liquid and gaseous inclusions within single grains (Mernagh & Liu 1991; Beyssac *et al.* 2002; Stefaniak *et al.* 2006; Bersani *et al.* 2009; Frezzotti *et al.* 2011). The Raman technique can also be used profitably in fission-track analysis

and detrital geochronology in general, to calibrate the crystallographic structure of apatite (Zattin *et al.* 2007) or to assess the degree of metamictization in zircon (Nasdala *et al.* 1996, 2001; Balan *et al.* 2001).

Finally, but perhaps most importantly, Raman spectroscopy allows us to reliably and routinely determine heavy minerals down to a few microns in size (Garzanti *et al.* 2011), and even to identify minerals in clay-rich muds (Villanueva *et al.* 2008), which is not feasible with standard optical techniques. Atmospheric particles can also be identified (Godoi *et al.* 2006; Potgieter-Vermaak *et al.* 2011). It is therefore unrivalled as a tool for the quantitative mineralogical analysis of fine-grained sediments – including suspended load in rivers, distal turbidites and wind-laid loess deposits – but has seldom been used so far because of operational difficulties (Blatt 1985; Totten & Hanan 2007). Raman spectroscopy can be readily and effectively applied in the mineralogical analysis of modern muds as well as ancient mudrocks (Andò *et al.* 2011). A whole frontier is thus opening up in provenance studies, given that mud represents a huge fraction of sediment transport, and mudrocks account for most of the stratigraphic

record (Blatt & Jones 1975) and are less affected by diagenetic dissolution than interlayered sandstones (Blatt & Sutherland 1969).

Raman mineral analysis (RaMAN)

Raman spectroscopy is an inelastic light-scattering technique widely used to study the vibrational properties of solids, liquids and gases (Nasdala *et al.* 2004; Frezzotti *et al.* 2012). The technique is routinely used in the study of economic ore deposits (Potgieter-Vermak 2007; Wells & Ramanaidou 2012) and in gemology (e.g. to identify whether diamonds have been treated artificially to change their colour and hence value; Bersani & Lottici 2010), but applications are wide ranging, including art and archaeology (Sendova *et al.* 2005; Vandenabeele *et al.* 2007; Aliatis *et al.* 2009), forensic investigations (Palenik 2007) and analysis of commercial products (pharmaceuticals, polymers, thin films, semiconductors, nanomaterials; Burgio & Clark 2001).

When monochromatic radiation strikes the molecules of a sample, the predominant mode of scattering is elastic (photons are scattered with unchanged energy and frequency). Occasionally, the molecule takes up energy from, or gives up energy to, the photons, which are scattered at a different wavelength (Stokes and anti-Stokes Raman scattering). It is this change in wavelength of the scattered photon (only 1×10^{-7} of the scattered light is Raman) that provides chemical and structural information.

The Raman technique can be applied to any mineral group, and is based on the identification of diagnostic peaks and comparison with reference spectra. The position of a Raman peak for a single crystal is constant, depending only on crystallographic structure and mineral chemistry. Detrital grains can thus be identified independent of their orientation. Peak intensity, however, is strongly dependent on crystal orientation relative to the polarization direction of the exciting and scattered light. Peak width yields images of crystallinity (e.g. metamictic zircon; Fig. 1). The ratio between the intensities of different peaks may be helpful in the identification of isomorphous series of isotropic minerals (e.g. garnets; Fig. 2).

The position of the peaks is influenced by grain size, as observed experimentally for crystals less than $10 \mu\text{m}$ in size, where the contribution of surface modes becomes significant, resulting in considerable lowering and increasing width of the Raman bands (Palmeri *et al.* 2009). In quartz, we have observed that such a shift is barely perceptible for grains coarser than *c.* $10 \mu\text{m}$, and is limited to 1 cm^{-1} in the $5\text{--}10 \mu\text{m}$ range. The effect is

therefore negligible for solid crystalline phases of sand to coarse-silt size, but becomes relevant when powders are analysed. The change in the Raman signal for powders is mainly due to a decrease in thermal conductivity; small grains are less able to dissipate the heat induced by the laser, and temperature therefore increases locally (Foucher *et al.* 2012). This problem can be circumvented by reducing the laser power and increasing the time for acquisition of the spectrum.

The Raman microscope

Raman analyses are performed with a standard optical microscope using either reflected or transmitted light, coupled with a laser source, an optical system to focus the incident beam, and a detector to analyse the scattered photons. The resolution of the spot size is $1 \mu\text{m}$ with the $\times 100$ objective, and single crystals down to a few microns in size can therefore be determined. Commonly used lasers range from the ultraviolet to the near-infrared, and can be interchanged automatically. Lasers in the $514\text{--}785 \text{ nm}$ range are best used to avoid problems caused by fluorescence effects. Solid-state lasers require minimum maintenance, and the cost of the spectrometer is affordable. Operations are handled by a computer with suitable software for data storage and processing. Modern instruments automatically find particles and focus on the centre of each one to collect Raman spectra. Accurate mineralogical maps along predefined grids and automatic point-counting can be achieved with imaging functions and a software-governed motorized *x-y* stage (Haskin *et al.* 1997; Nasdala *et al.* 2012). In this way, survey scans of representative areas in thin sections and heavy-mineral mounts can be obtained efficiently.

Raman spectra acquisition and mineral identification

The collection of a single spectrum requires an acquisition time ranging from just a second for minerals with good Raman response (quartz, carbonates, zircon) to about a minute for minerals with poor Raman signal (e.g. phyllosilicates). The poor signal of Fe–Ti–Cr oxides can be improved by mounting opaque grains directly on pin stubs to avoid interference of the bonding resin (Fig. 3). Dark and strongly pleochroic minerals (e.g. amphibole) may have a marked fluorescence emission that hides Raman features. Fluorescence effects can be avoided by selecting a suitable laser excitation wavelength.

Because shifting of Raman peaks can be produced by heating of metallic parts during prolonged

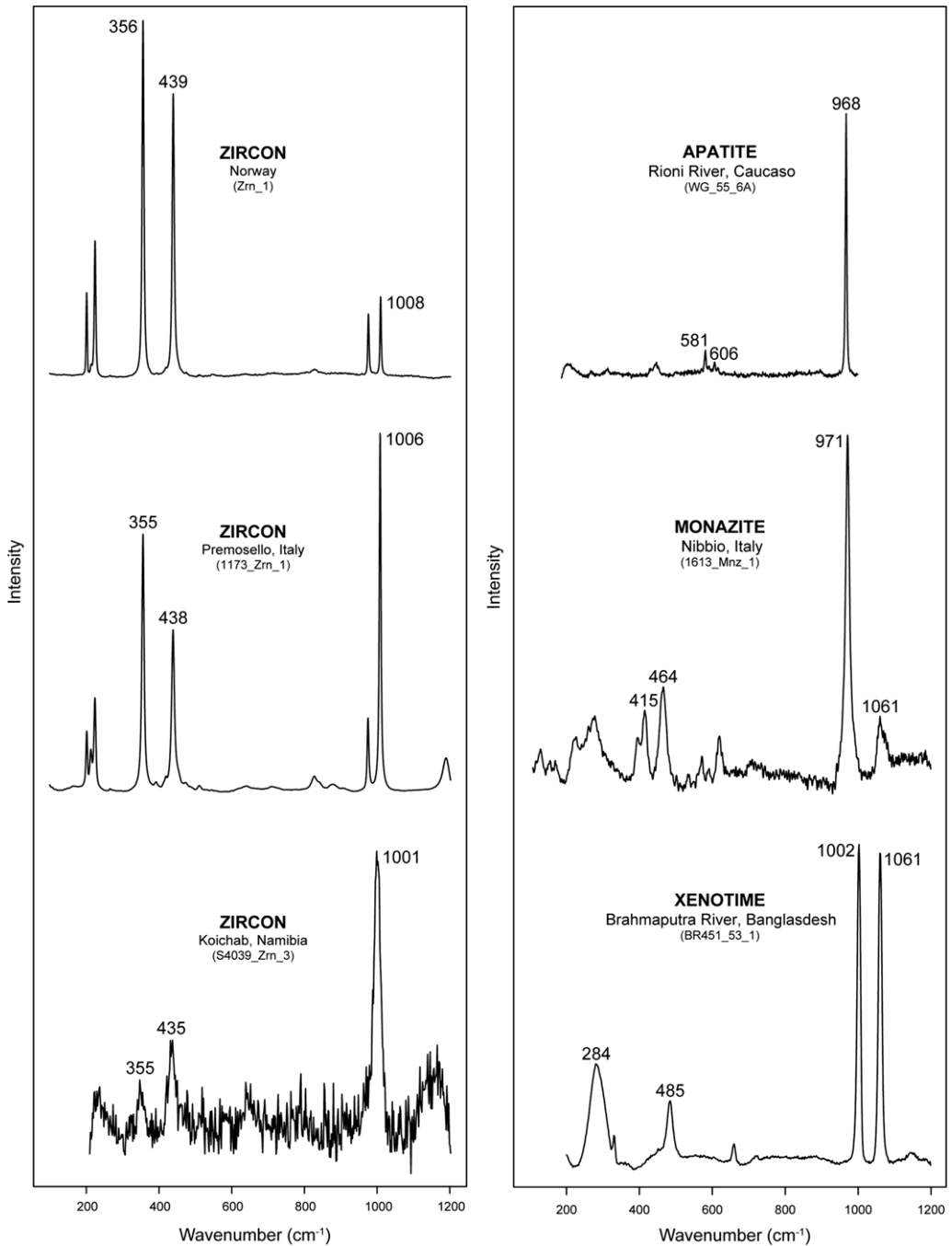


Fig. 1. Raman assessment of the degree of metamictization in zircon and discrimination of detrital phosphates.

Well-ordered zircons show distinct, narrow internal and external vibrational modes between 200 and 1010 cm^{-1} . With increasing radiation damage, all main Raman bands decrease in intensity and become increasingly broader, and show a notable shift towards lower wavenumbers (Nasdala *et al.* 2001). Phosphates are strong Raman scatterers. For all figures, detailed information on the lasers used and the origin of the analysed minerals are provided in the Supplementary material.

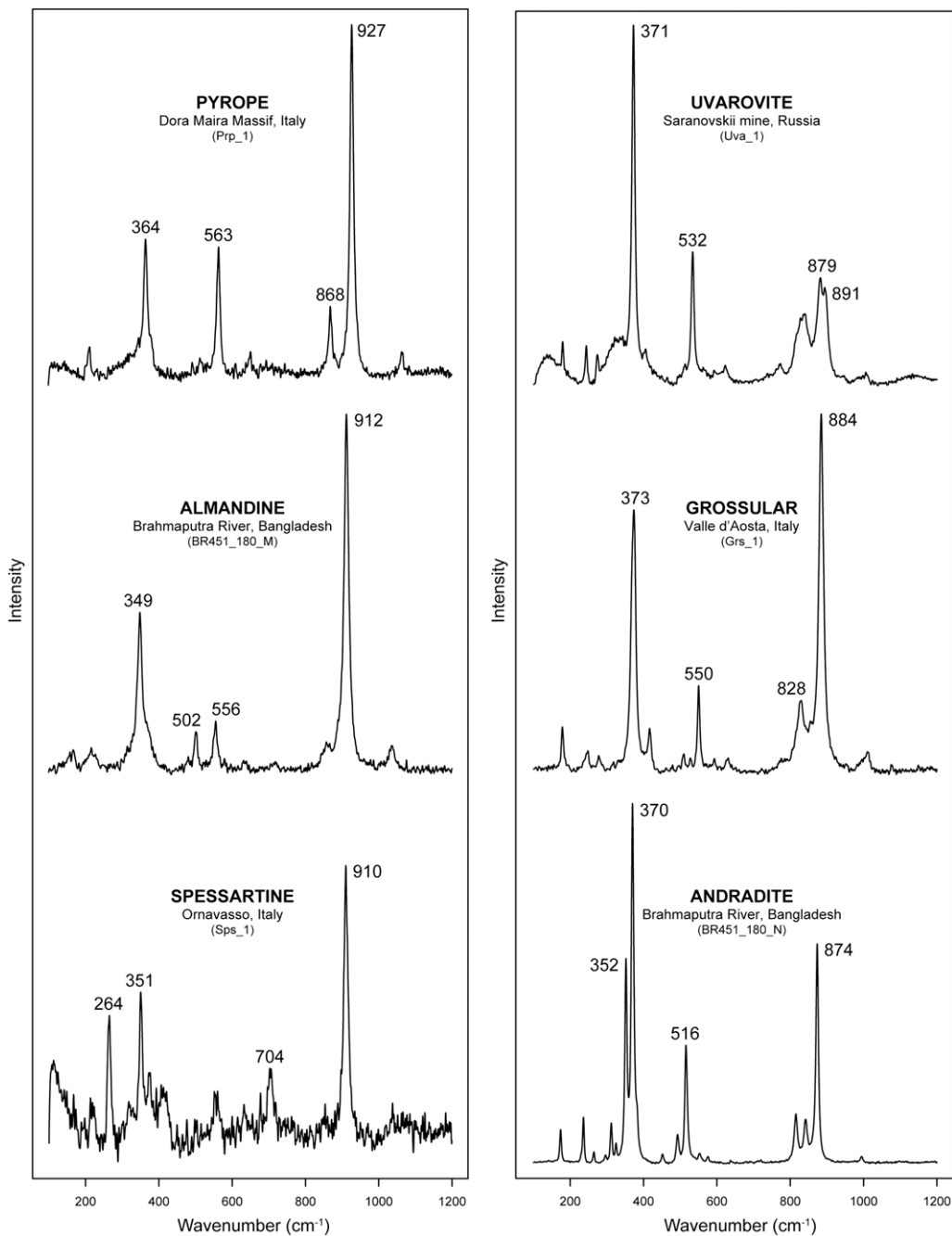


Fig. 2. Discriminating within the isomorphous series of garnets. Pyralspite and ugrandite garnets can be distinguished by the position of peaks found at high frequencies and caused by Si–O stretching modes ($873\text{--}880\text{ cm}^{-1}$ in ugrandites, $907\text{--}926\text{ cm}^{-1}$ in pyralspites; Bersani *et al.* 2009).

use, spectra have to be calibrated frequently (e.g. hourly by using, as a reference, the signal from a silicon wafer at 520.7 cm^{-1} , or ‘plasma lines’ in

opaque minerals with metallic lustre, or the position of characteristic lines for each laser). Because diagnostic phonon modes are found in the low Raman-

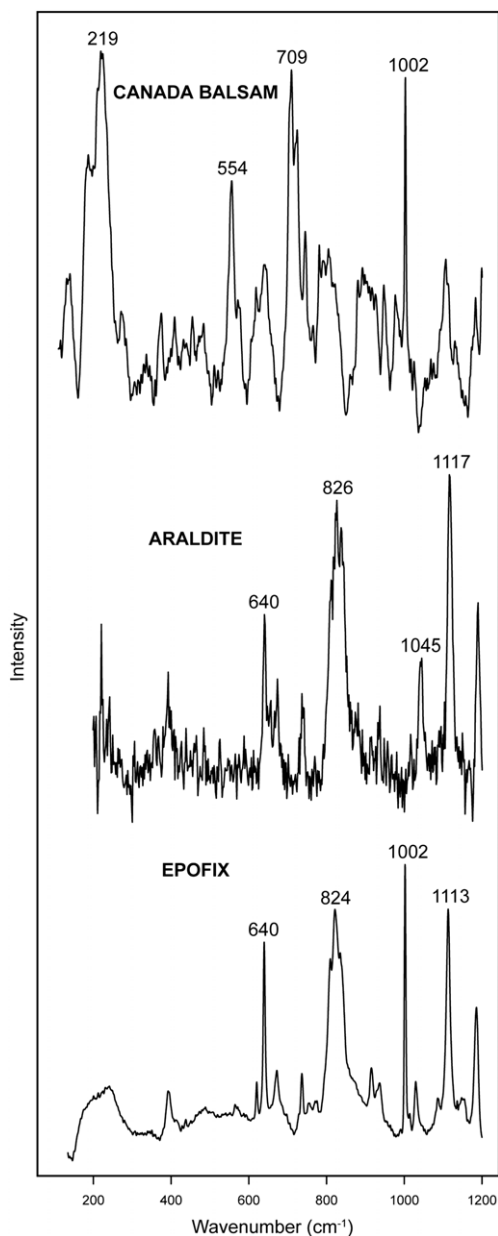


Fig. 3. Raman signal of common bonding resins. The spectrum of the bonding resin needs to be subtracted before interpreting the Raman spectrum obtained, because the most intense peaks may interfere with the diagnostic peaks of heavy minerals, particularly in the spectral region above 600 cm^{-1} .

shift region (e.g. $180\text{--}520\text{ cm}^{-1}$ for quartz and feldspars) as well as in the high Raman-shift region ($>800\text{ cm}^{-1}$ for carbonates, phosphates, garnet,

zircon), calibration with a pure calcite spar, end-member garnet or non-metamictic zircon is also advised. Modern acquisition systems have a self-calibrating device that operates before each measure and takes the whole spectral region into account. It is advisable to adopt a configuration that allows the collection of signals in low-frequency regions between 50 and 150 cm^{-1} , where diagnostic vibrational modes allowing more accurate identification of mineral species (e.g. feldspars, carbonates) may be present.

Detrital minerals are determined by comparison of the obtained Raman peaks with reference spectra reported in the literature (e.g. Wang *et al.* 2004 for Fe–Ti–Cr oxides; Kolesov & Geiger 1998 and Geiger 2008 for garnets; Freeman *et al.* 2008 for feldspars) and mineralogical databases available online (e.g. www.irug.org, www.ruff.info, Downs 2006; Parma University, www.fis.unipr.it/phevix/ramandb.php; Lyon University, www.ens-lyon.fr/LST/Raman/index.php; Romanian Database, <http://rdrs.uaic.ro/>). Additional in-house spectra obtained from minerals of precisely known specific chemical composition are commonly and profitably used.

In order to allow the comparison of Raman spectra with optical properties observed under both a stereomicroscope and a transmitted-light microscope, single grains within the counted area of a heavy-mineral slide or thin section must be encircled with a marker pen or identified on a photograph and numbered. Combining optical observations under the microscope and Raman analyses allows us to determine how peak intensities vary with crystal orientation relative to the laser vibrational direction, and to independently identify any anisotropic mineral from the crystal face under scrutiny. In general, prismatic faces elongated parallel to the *c*-axis are most commonly observed in grain mounts, whereas sections randomly cut oblique to the *c*-axis are typically observed in thin sections.

Operational conditions of our experiments

Non-polarized micro-Raman spectra were obtained in nearly backscattered geometry with two different instruments and four different laser wavelengths at CNR-ICVBC Milano, University of Parma and University of Milano-Bicocca.

The 632.8 nm line of a He–Ne laser and the 488 nm line of an Ar^+ laser were used for excitation with a Jobin-Yvon Horiba LabRam apparatus, equipped with an Olympus microscope with $\times 10$, $\times 50$ and $\times 100$ objectives and a motorized *x–y* stage. The system was calibrated using the 520.7 cm^{-1} Raman silicon band before each experimental session. Spectra were generally collected with counting times ranging between 60 and 180 s.

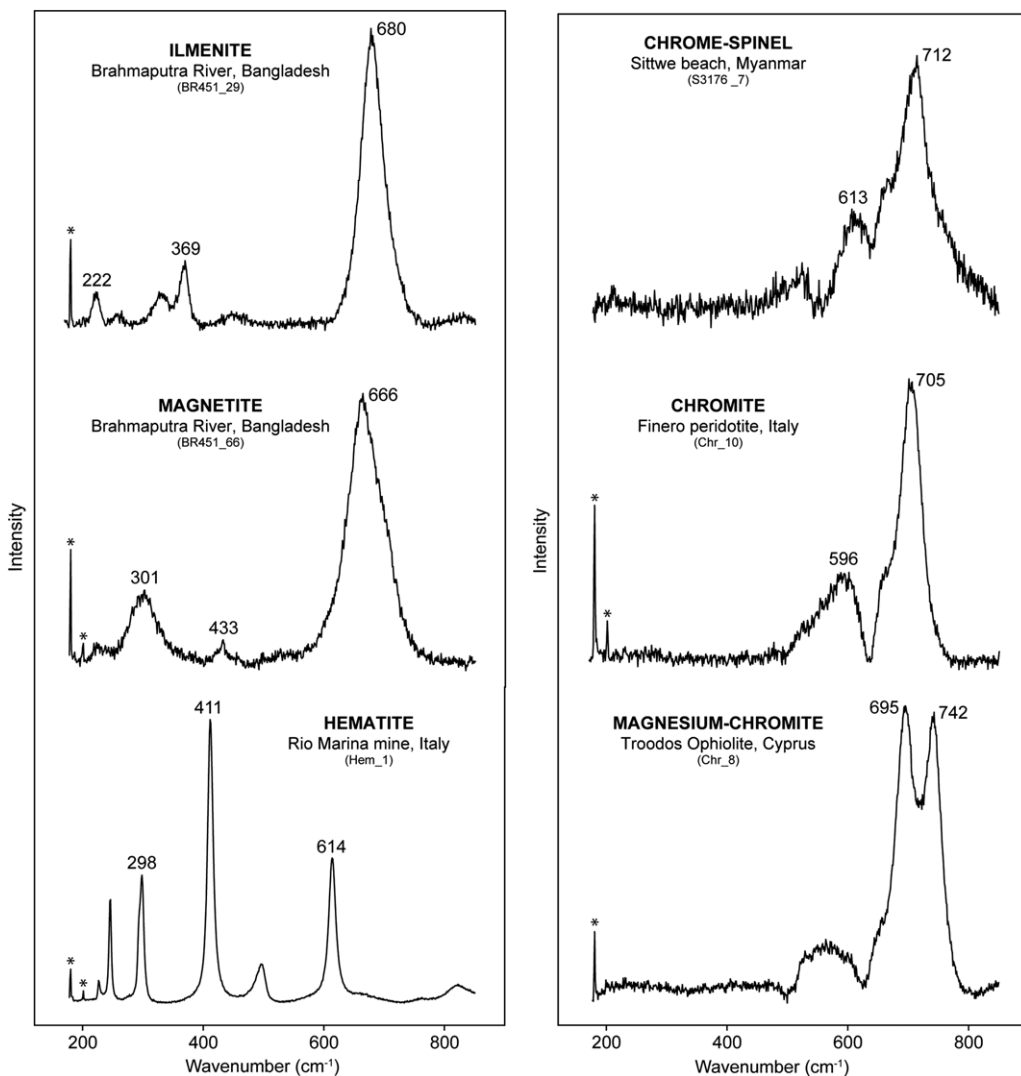


Fig. 4. Raman discrimination of opaque and non-opaque Fe–Ti–Cr oxides. The position and shape of the strongest peak in the 660–680 cm^{-1} spectral region (A_{1g} mode) is most useful for assessing Fe^{3+} –Ti–Cr–Al substitutions in the magnetite-ulvöspinel, ulvöspinel-chromite and chromite-spinel series. Minor peaks in the range 300–600 cm^{-1} also assist in identification (Wang *et al.* 2004). *He–Ne, 633 nm; plasma lines, 180, 202 cm^{-1} .

The 785 nm line of a NIR laser and the 532 nm line of a solid-state laser were used for excitation with a Bruker Senterra dispersive spectrometer, equipped with an Olympus microscope with $\times 20$, $\times 50$ and $\times 100$ objectives and a motorized x – y stage. The system was automatically calibrated using the Raman frequencies of an internal neon lamp before each measurement. Spectra were collected with counting times ranging between 90 and 180 s.

For both instruments, the minimum lateral and depth resolution was set to *c.* 2 μm with a confocal hole. Laser power was controlled by means of a series of density filters in order to avoid heating effects. The wavenumbers of the Raman bands were then determined by fitting with Voigt functions using the LabSpec software, after polynomial background removal. The uncertainty on the measured wavenumbers was estimated at less than 1 cm^{-1} , which allowed us to confidently distinguish

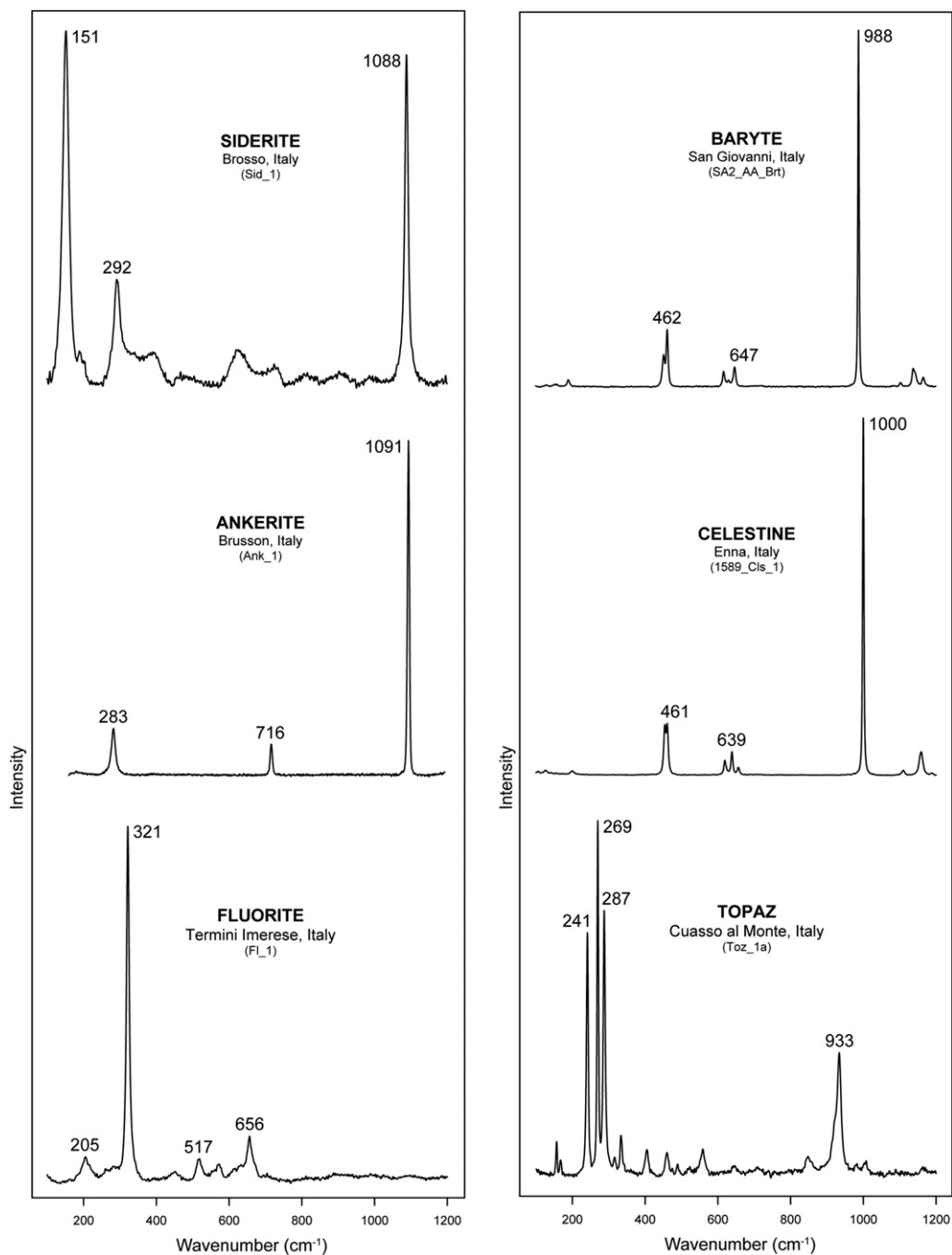


Fig. 5. Raman discrimination of heavy carbonates, sulphates and F-bearing minerals. Carbonates and sulphates are strong Raman scatterers. Carbonates display Raman modes at $c. 1100 \text{ cm}^{-1}$ due to the symmetric stretching vibration (ν_1) of the CO_3 group. The positions of their lattice modes over the range $100\text{--}350 \text{ cm}^{-1}$ are also diagnostic. Sulphates display Raman modes at $c. 1000 \text{ cm}^{-1}$ due to the symmetric stretching vibration (ν_1) of the SO_4 group.

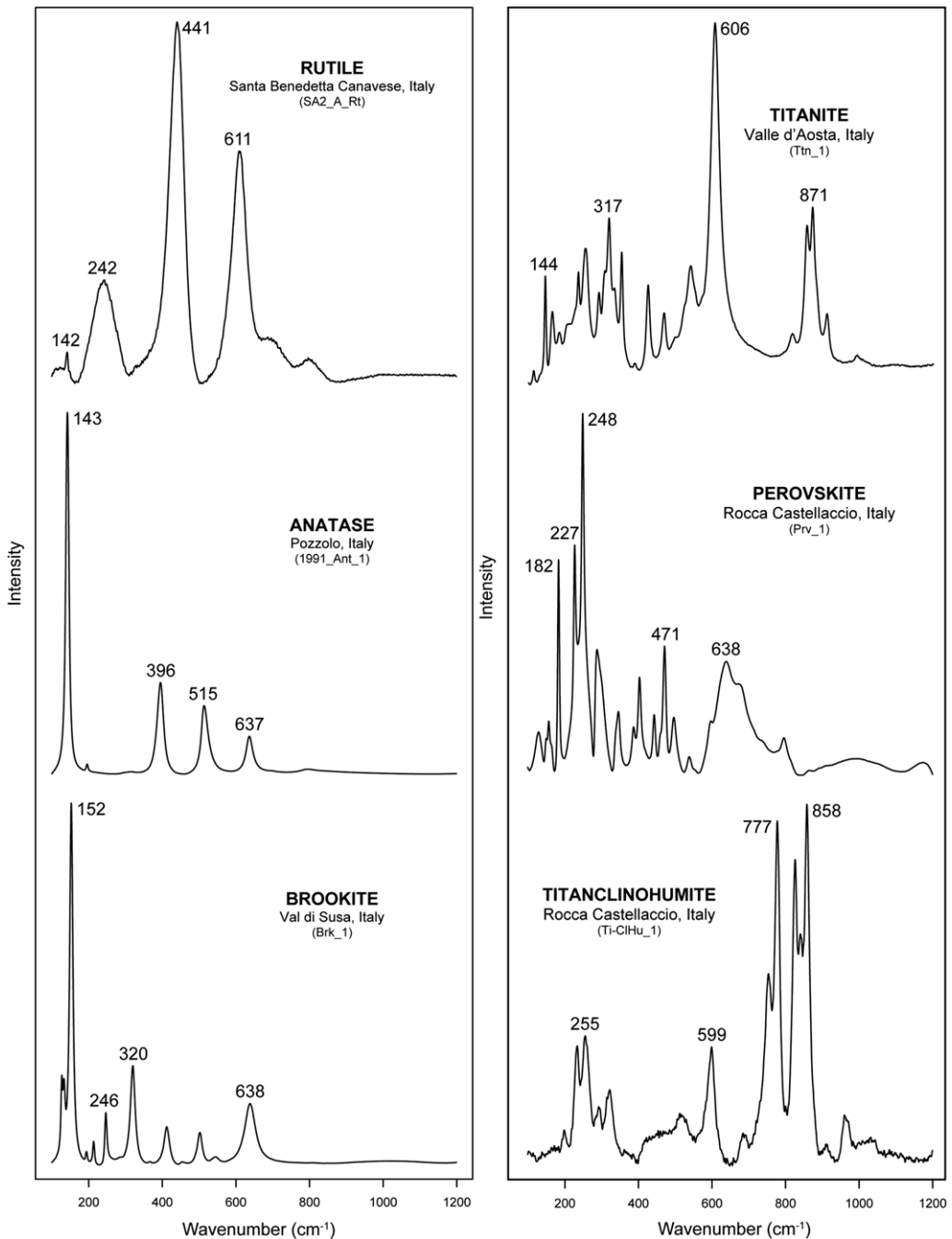


Fig. 6. Raman discrimination of Ti-oxide polymorphs and Ti-bearing minerals. Note the marked differences in rutile, anatase and brookite spectra.

mineralogical species even within isomorphous series (e.g. garnets, Bersani *et al.* 2009). Grains were individually selected for analysis, and time and focus

were set by the operator. At least three different spots were analysed for each grain, and the best spectrum obtained was selected for identification.

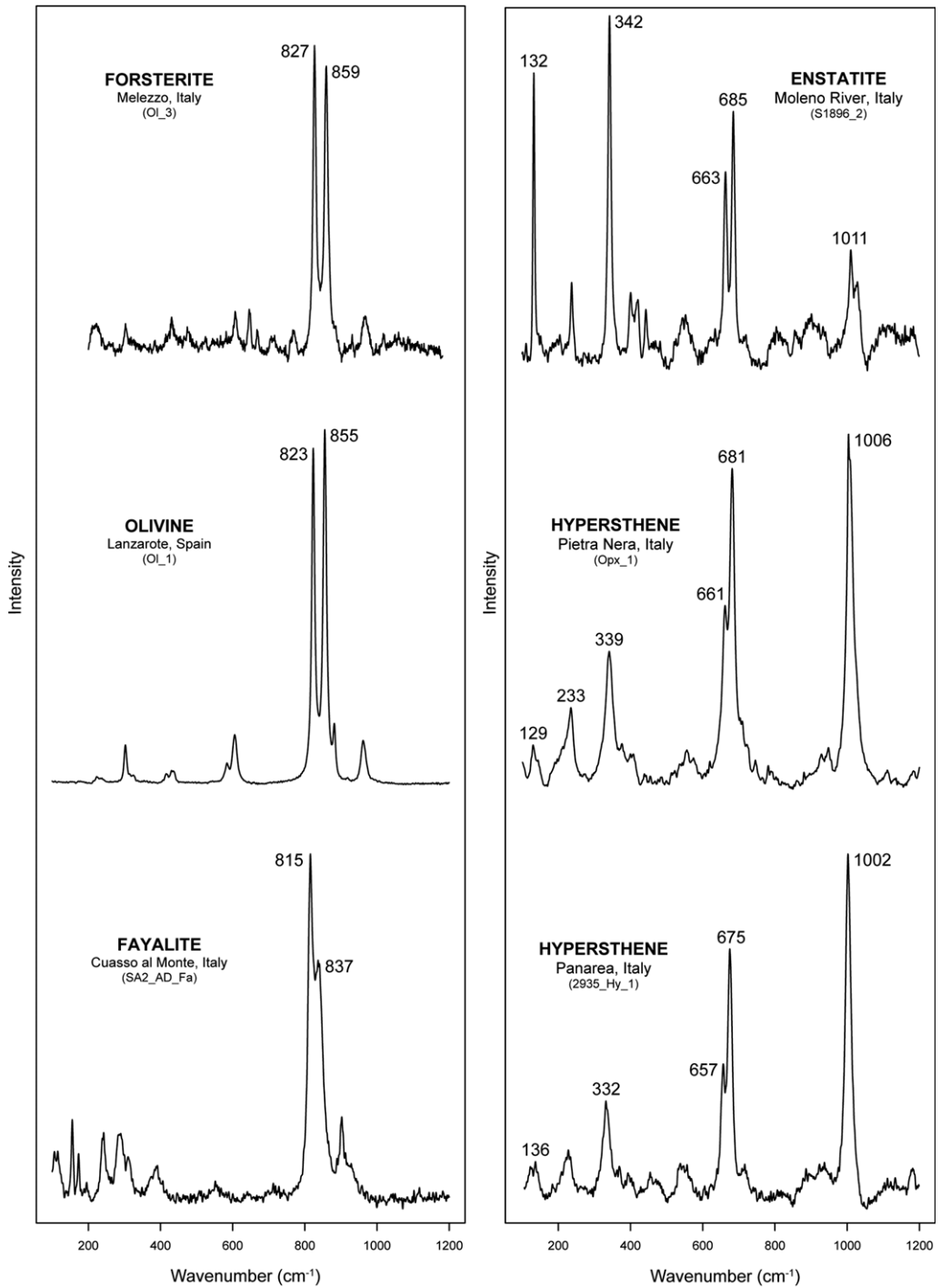


Fig. 7. Raman discrimination of olivines and orthopyroxenes. The very good correlation between cation substitution (Mg/Fe + Mg) and the wavenumbers of the SiO₄ main bands allows accurate determination of the chemical composition of olivines (Guyot *et al.* 1986; Kübler *et al.* 2006).

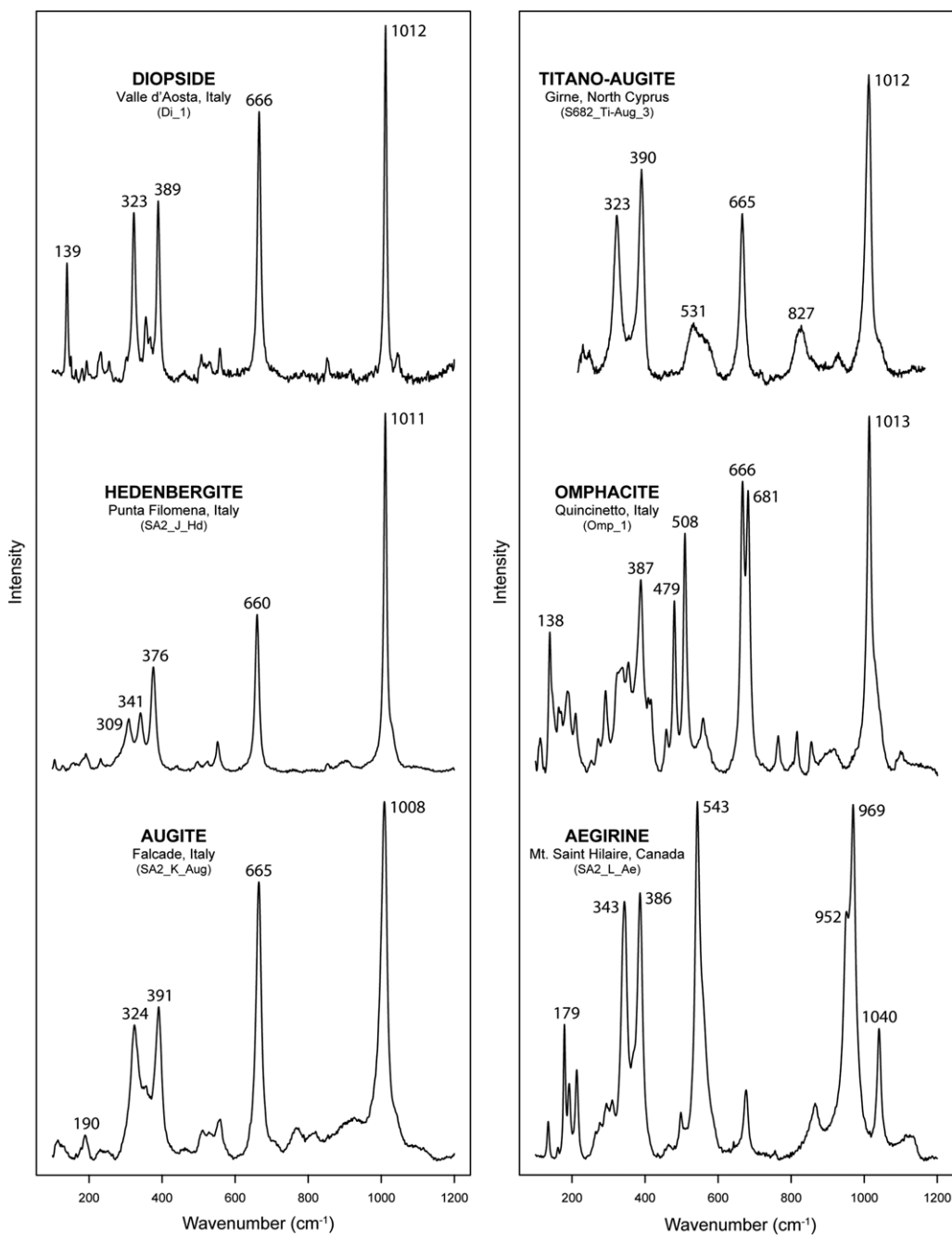


Fig. 8. Raman discrimination of clinopyroxenes. Pyroxenes can be distinguished by the number of bands in the 600–700 cm^{-1} region. Clinopyroxenes have one single band, whereas orthopyroxenes have two bands (Fig. 7).

RaMAN in provenance studies

Raman mineral analysis allows us to confidently identify dubious detrital minerals independently

of their size and orientation. During counting of heavy-mineral mounts or thin sections, grain types that cannot be specifically determined are usually assigned to generic groups (i.e. opaques, turbid

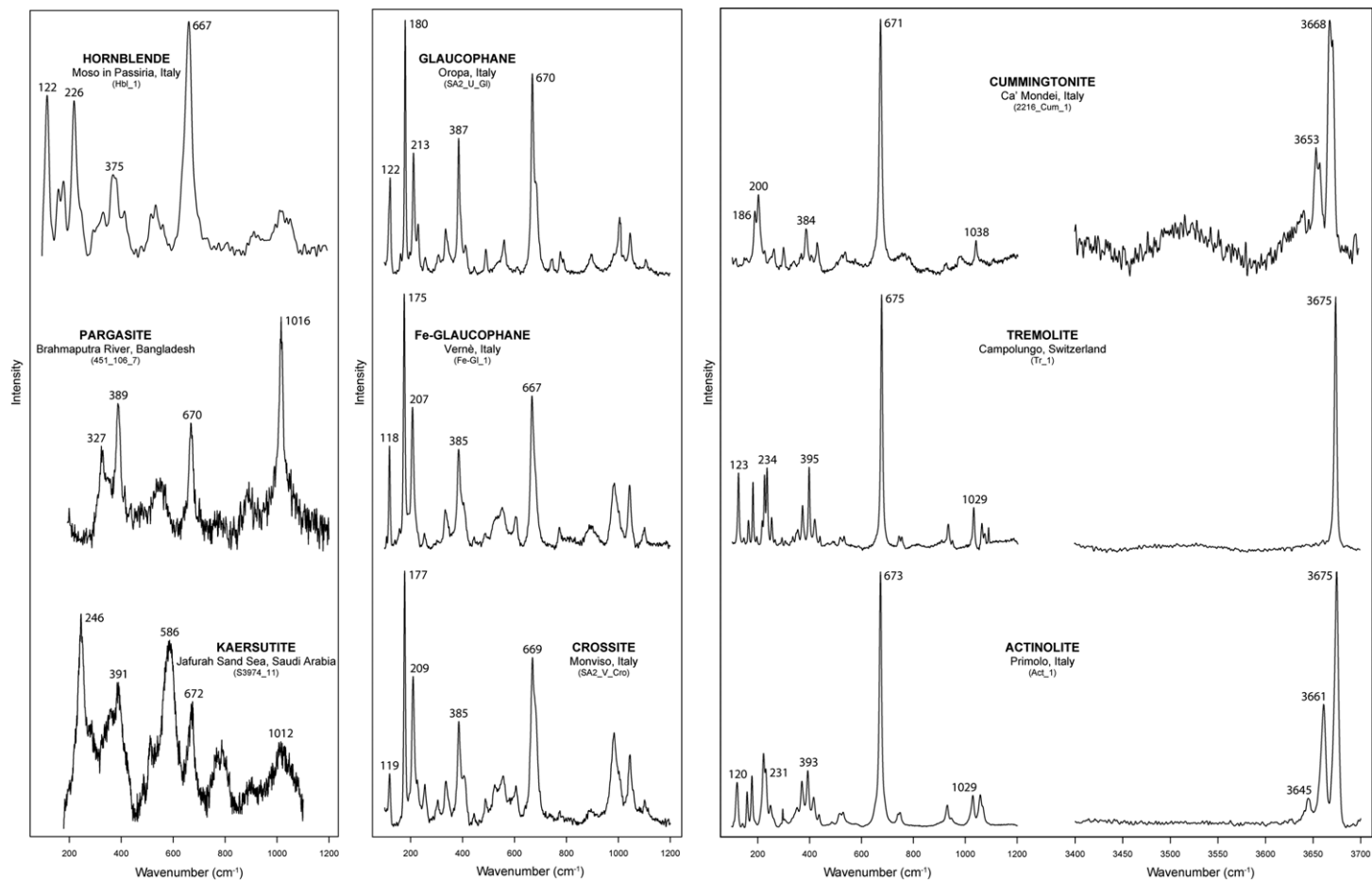


Fig. 9. Raman discrimination of amphiboles. Because they are very weak Raman scatterers due to both their dark colour and the low polarizability of their Si–O bonds, identification of amphiboles may be difficult. The diagnostic position and shape of the more intense OH stretching bands (frequencies between 3600 and 3700 cm^{-1}) is particularly helpful (as shown for cummingtonite, tremolite and actinolite).

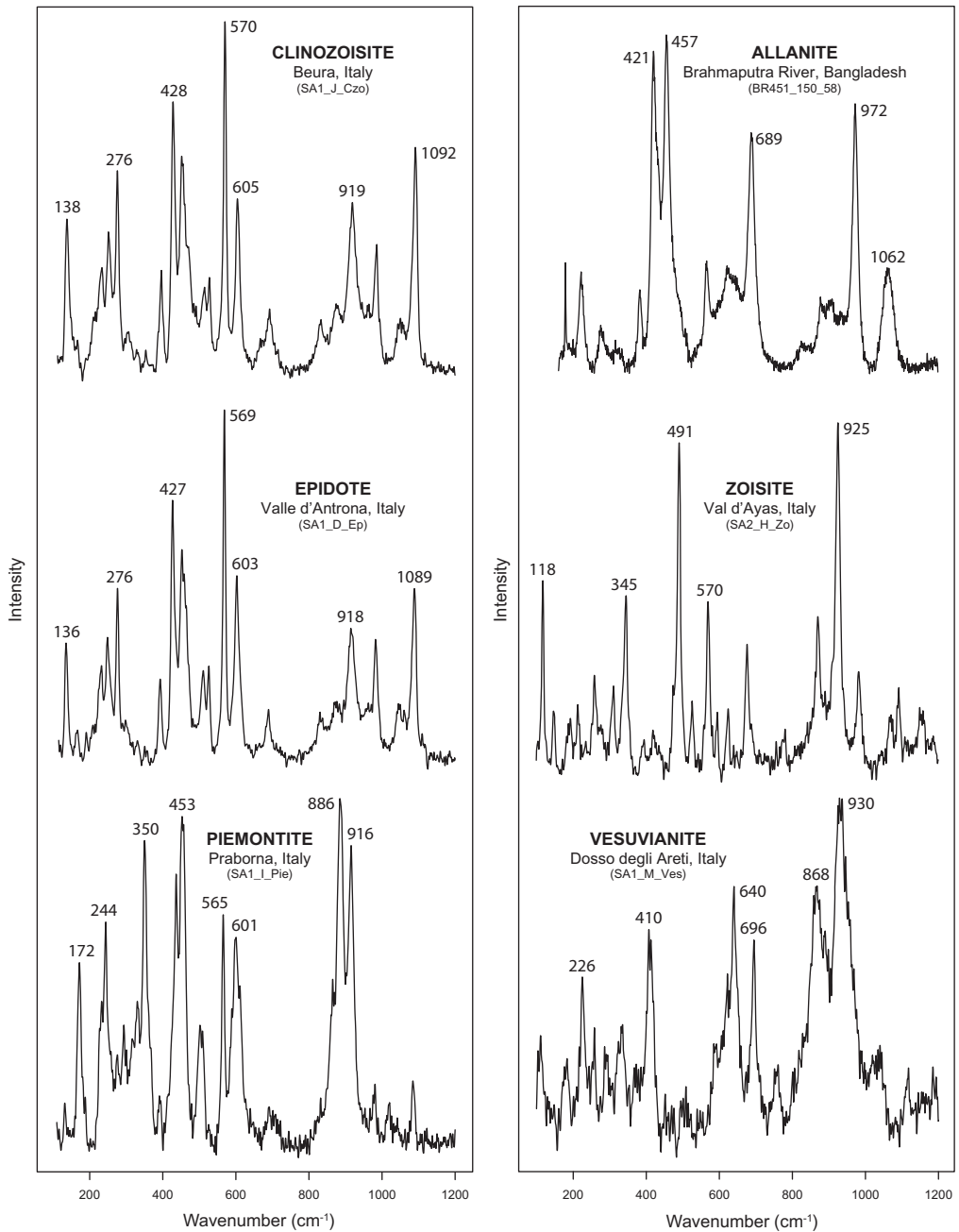


Fig. 10. Raman discrimination of epidote-group minerals and vesuvianite. The characteristic abundance of vibrational modes in sorosilicates facilitates distinction from other silicates (e.g. pyroxenes).

grains, alterites, undetermined rock fragments) and generally neglected in subsequent provenance considerations, which may result in a partial and seriously biased description and interpretation of the detrital assemblage.

The RaMAN technique, instead, allows us to identify various types of opaque and transparent accessory minerals as well as altered grains of uncertain origin, and even to quantitatively or semi-quantitatively analyse the chemistry of solid

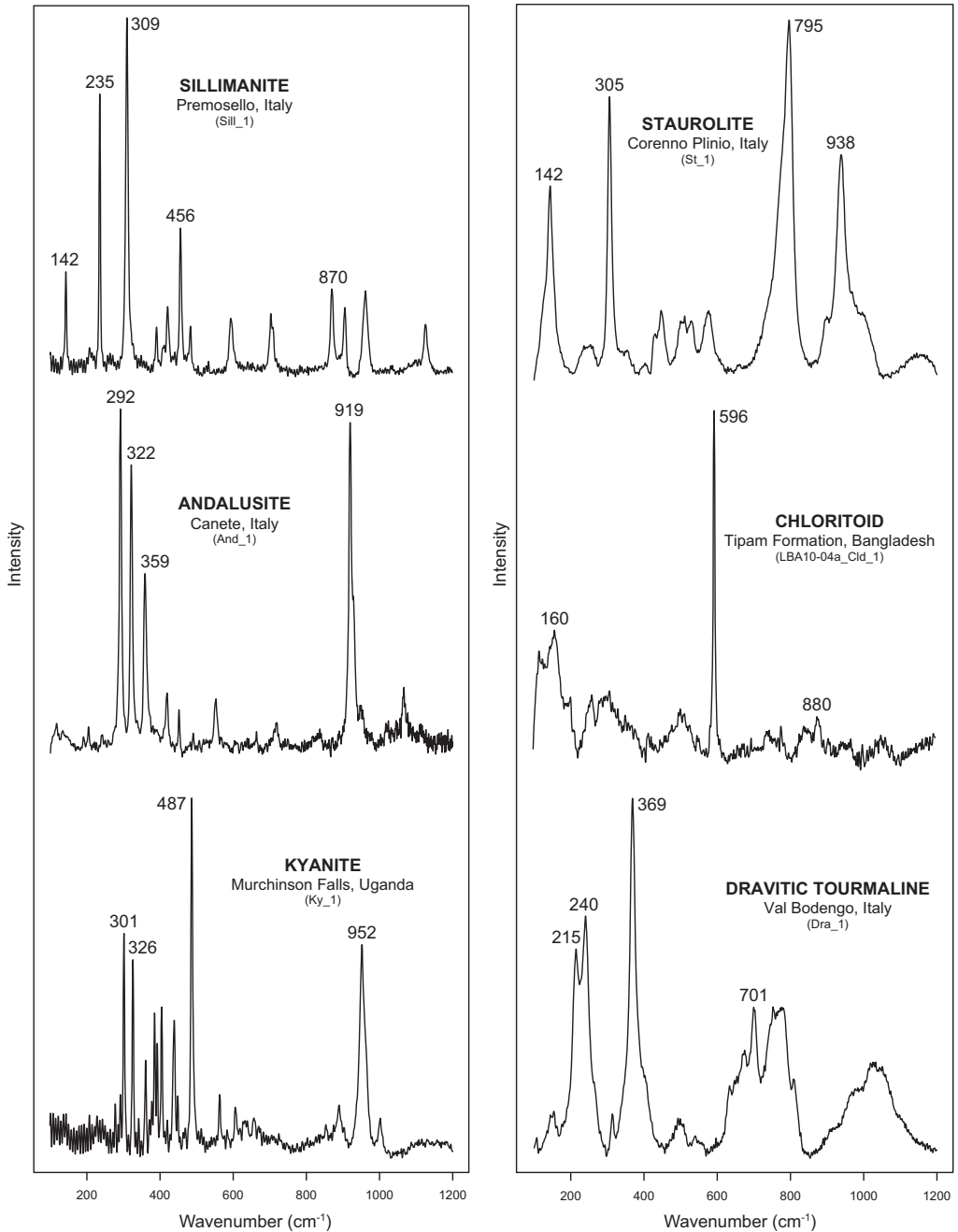


Fig. 11. Raman discrimination of minerals from metasedimentary rocks.

solutions and isomorphic series (amphiboles, pyroxenes, garnets, feldspars, carbonates). Among opaque accessory minerals, which may be strongly concentrated in placer deposits of economic

interest (Worobiec *et al.* 2007) and are particularly relevant for both provenance (Basu & Molinaroli 1989) and settling-equivalence studies (Garzanti *et al.* 2008), magnetite, ilmenite or chromite can

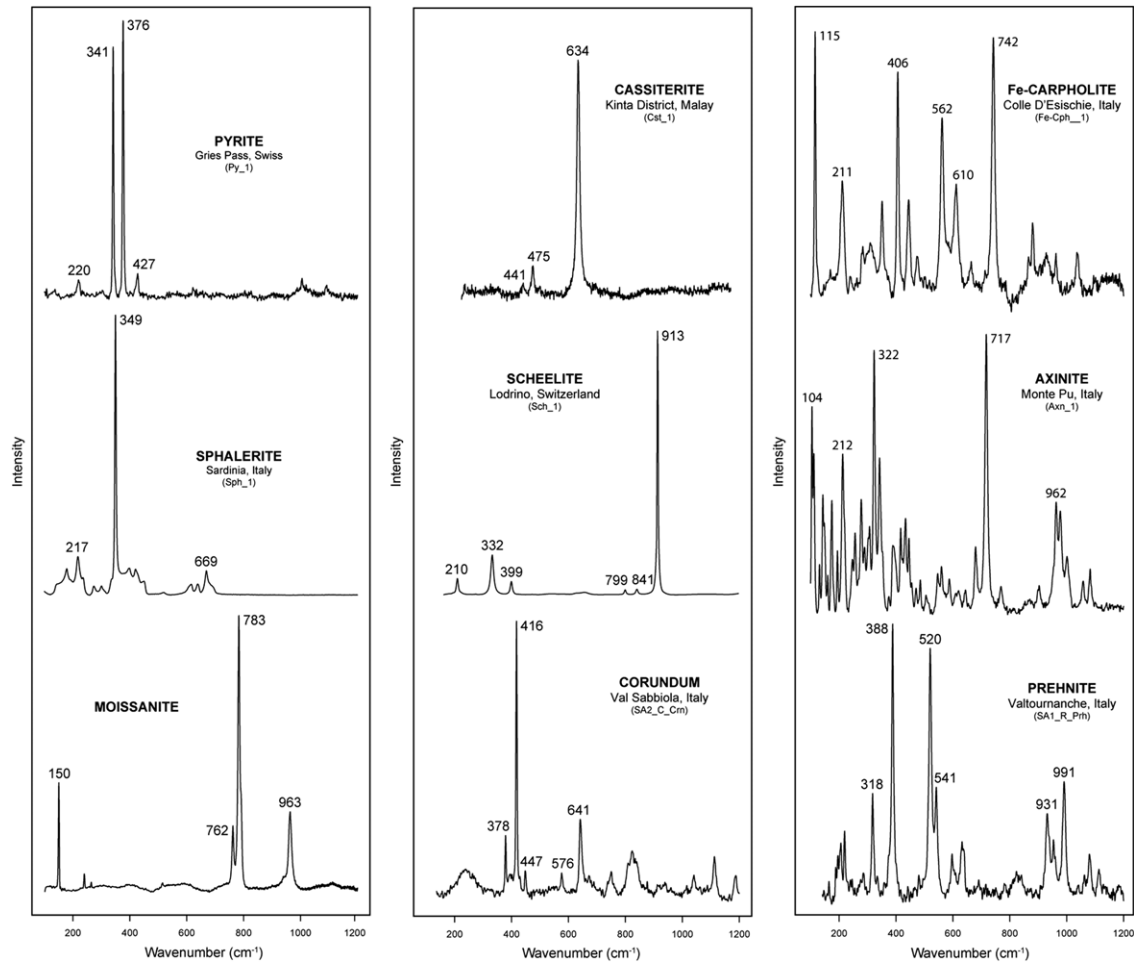


Fig. 12. Raman discrimination of other heavy minerals. The rare rock-forming minerals corundum and moissanite (e.g. Di Piero *et al.* 2003) are commonly used as abrasive paste, and may thus occur in heavy-mineral slides due to anthropic contamination.

be discriminated (Fig. 4; Shebanova & Lazor 2003; Garzanti *et al.* 2010). Among rock fragments of uncertain origin, felsic volcanic grains containing anhedral feldspars can be reliably distinguished from impure chert and cherty mudstones, and limestone from dolostone. Of the detrital feldspars, which if untwinned and <100 µm in size are not invariably easy to identify under a polarizing microscope, we can readily detect Na-plagioclase from Ca-plagioclase, for example, and detrital orthoclase or microcline cores from adularia syntaxial overgrowths. Untwinned feldspars can be easily discriminated from quartz in silt-sized sediments, and sanidine from anorthoclase and plagioclase in volcanic rock fragments. Various types of phyllosilicates useful for provenance (e.g. phlogopite) or environmental diagnosis (e.g. clay minerals, glauconite; Ospitali *et al.* 2008) can be determined, as well as authigenic tectosilicates, phyllosilicates, carbonates or sulphates (Wang *et al.* 2006), which are particularly useful in the reconstruction of post-depositional evolution during burial, lithification and final exhumation (Fig. 5).

RaMAN in heavy-mineral studies

Raman mineral analysis allows us to efficiently solve a number of problems found routinely in traditional heavy-mineral studies, but that cannot be confidently dealt with under the polarizing microscope, even by an experienced operator. Moreover, with Raman spectroscopy we can readily distinguish single phases and solid solutions of opaque Fe–Ti–Cr oxide grains, found in variable amounts in virtually all heavy-mineral separates (Fig. 4). We can distinguish among Ti-oxide polymorphs (Fig. 6), identify altered minerals (particularly common in sediments derived from very low-grade metasedimentary source rocks), and analyse authigenic heavy minerals (which may occur in abundance in both ancient sandstones and in polycyclic sediments derived from them).

Even the identification of unweathered transparent heavy minerals is not invariably straightforward under the optical microscope. This is particularly true for colourless grains that cannot be easily oriented because they lack cleavage and evident crystal faces, for rounded high-relief and high-birefringence grains (e.g. REE phosphates; Silva *et al.* 2006) or for fibrous grains displaying incomplete extinction. Orientation problems are most serious in the study of aeolian sands, where detrital minerals are commonly transformed into quasi-perfect spheres.

With Raman spectroscopy we can rapidly solve the thorny identification problems routinely encountered in optical heavy-mineral analysis, and

reliably distinguish among colourless magnesian minerals (forsterite, enstatite, diopside, tremolite, Mg-cummingtonite, Mg-anthophyllite; Figs 7–9), for instance, or among pale-green weakly ferri-ferrous minerals with intermediate birefringence (e.g. olivine, pigeonite, Fe-diopside, omphacite, actinolite, Fe-anthophyllite, grunerite, Fe-poor epidote; Figs 7–10). RaMAN can thus efficiently solve all long-standing problems in heavy-mineral analysis, including the following (Mange & Maurer 1992):

- (1) olivine v. enstatite or prismatic sillimanite (Figs 7 & 11);
- (2) anthophyllite v. fibrolitic sillimanite (Figs 9 & 11);
- (3) prismatic sillimanite v. apatite or topaz (Figs 1, 5 & 11);
- (4) baryte and celestite v. kyanite (Figs 5 & 11);
- (5) pale-green augite v. epidote or clinzoisite (Figs 8 & 10);
- (6) brown hornblende v. allanite (Figs 9 & 10);
- (7) colourless zircon v. monazite, xenotime or titanite (Figs 1 & 6);
- (8) metamictic zircon v. rutile, cassiterite or sphalerite (Figs 1, 6 & 12).

In varietal studies (Morton 1985; Mange & Wright 2007), Raman spectroscopy represents a particularly powerful, complementary time-saving technique (Andò *et al.* 2009), because precious chemical information can be obtained rapidly, on many grains, and directly on heavy-mineral mounts without further preparation. We can thus quantitatively or semi-quantitatively assess the chemistry of isomorphic series for detrital spinels, olivines or garnets (Guyot *et al.* 1986; Wang *et al.* 2004; Kübler *et al.* 2006; Bersani *et al.* 2009; Figs 2, 4 & 7), and readily identify silicate varieties such as sodic clinopyroxenes or amphiboles (Figs 8 & 9). Raman spectroscopy also offers an opportunity to:

- (1) identify rare grains occasionally encountered in heavy-mineral slides or thin sections;
- (2) investigate gaseous, liquid and solid inclusions in single detrital minerals (e.g. apatite, zircon, micas);
- (3) calibrate the apatite chemistry and assess the degree of metamictization in zircon;
- (4) assess varieties in REE-bearing minerals (e.g. Ce-allanite v. La-allanite or Y-allanite);
- (5) investigate anisotropic crystal behaviour for physical or chemical processes (e.g. weathering, diagenetic dissolution);
- (6) investigate natural photoluminescence in garnet, tourmaline and monazite (Bersani *et al.* 2012; Lenz *et al.* 2012);
- (7) distinguish among minerals containing OH⁻ groups (e.g. amphiboles, phyllosilicates; Wang *et al.* 1988; Frezzotti *et al.* 2012).

Moreover, RaMAn can be used to investigate the nature of anisotropic domains (e.g. in garnets), strain effects or the metamictic effect on the lattice structure produced by radiogenic α -decay (Nasdala *et al.* 2012).

Conclusions

Traditional heavy-mineral analysis under the microscope provides us with a wealth of detailed information on the geology of source areas as well as on physical and chemical processes that took place subsequently during the sedimentary cycle. However, its full efficacy is hampered by limits in the identification of detrital grains that are barely overcome even by operators with ability and experience. Opaque minerals or turbid altered grains are generally impossible to determine under the transmitted-light petrographic microscope, and consequently the information they potentially convey is overlooked and lost. Furthermore, in the case of unweathered, colourless minerals of uncertain orientation, only a tentative determination may be obtained, particularly if grains are well-rounded or silt-sized. The best tool to overcome all of these routinely encountered obstacles is the Raman spectroscope, which, in a few seconds, allows us to obtain, even on the very same grain mounts or thin sections and without any specific additional preparation, a spectrum whose frequencies are diagnostic not only of the different mineralogical species, but also of subtle variations in the chemical composition and crystallographic structure of each detrital mineral. In several cases, Raman spectroscopy can provide virtually the same information on the chemistry of detrital minerals as obtained by more expensive and less user-friendly instruments such as the electron microprobe (Smith 2005; Bersani *et al.* 2009), and in some cases even information that cannot be easily obtained otherwise (e.g. on the nature of solid or fluid inclusions, the degree of metamictization or the occurrence of OH⁻ groups). The Raman technique is also quite helpful in the identification of minute features of minerals most widely used in detrital geochronology (e.g. zircon, apatite, rutile), allowing us to discriminate among different apatite or zircon types that respond differently to chemical attack or geochronological analysis (Balan *et al.* 2001; Nasdala *et al.* 2001; Zattin *et al.* 2007; Malusà *et al.* 2013).

Last, but not least, Raman spectroscopy allows us to reliably determine detrital minerals as fine-grained or fine silt. Quantitative heavy-mineral investigation of suspended load in rivers, distal turbidite deposits and wind-laid loess becomes possible, with the same precision level reached

in provenance analysis of sand-sized sediments (Andò *et al.* 2011). This powerful technique thus provides us with a new user-friendly key to unlock the sedimentary record preserved in ancient clastic wedges, a conspicuous part of which is represented by silty mudrocks. By considering not only the coarse fraction, which is easier to handle and analyse in the laboratory, but the entire sediment flux conveyed through fluvial–deltaic–turbiditic systems, we can better constrain how and to what extent sediment composition is modified physically and chemically during transfer from detrital sources to depositional sinks, and thus calculate sediment budgets more accurately and achieve a deeper understanding of sedimentary processes in general. Borrowing our conclusive words from the seminal article by Raman (1928, p. 376), ‘we are obviously only at the fringe of a fascinating new region of experimental research, which promises to throw light on diverse problems. . . . It all remains to be worked out’!

We heartily thank D. Bersani (University of Parma), I. Aliatis (CNR-ICVBC Milano), A. Paleari (University of Milano-Bicocca) and P. Censi (University of Palermo) for their great help and advice through the years. M. Mange, P. Vignola, P. Gentile, A. Castiglioni, G. Castiglioni, M. Marzini, R. Sala and A. Resentini provided minerals from their collections and technical support. Discussions with, and insightful comments by, L. Nasdala, O. Beyssac and C. Lenz at EGU 2012 are gratefully acknowledged.

References

- ALIATIS, I., BERSANI, D. *ET AL.* 2009. Green pigments of the Pompeian artists’ palette. *Spectrochimica Acta, Part A*, **73**, 532–538.
- ANDÒ, S., BERSANI, D., VIGNOLA, P. & GARZANTI, E. 2009. Raman spectroscopy as an effective tool for high-resolution heavy-mineral analysis: examples from major Himalayan and Alpine fluvio-deltaic systems. *Spectrochimica Acta, Part A*, **73**, 450–455.
- ANDÒ, S., VIGNOLA, P. & GARZANTI, E. 2011. Raman counting: a new method to determine provenance of silt. *Rendiconti Lincei*, **22**, 327–347.
- BALAN, E., NEUVILLE, D. R., TROCELLIER, P., FRITSCH, E., MULLER, J. P. & CALAS, G. 2001. Metamictization and chemical durability of detrital zircon. *American Mineralogist*, **86**, 1025–1033.
- BASU, A. & MOLINAROLI, E. 1989. Provenance characteristics of detrital opaque Fe–Ti oxide minerals. *Journal of Sedimentary Research*, **59**, 922–934.
- BERSANI, D. & LOTTICI, P. P. 2010. Applications of Raman spectroscopy to gemology. *Analytical and Bioanalytical Chemistry*, **397**, 2631–2646.
- BERSANI, D., ANDÒ, S., VIGNOLA, P., MOLTIFIORI, G., MARINO, I. G., LOTTICI, P. P. & DIELLA, V. 2009. Micro-Raman spectroscopy as a routine tool for garnet analysis. *Spectrochimica Acta, Part A*, **73**, 484–491.

- BERSANI, D., PETRIGLIERI, J. R., ANDÒ, S. & LOTTICI, P. P. 2012. Identification of impurities in gemological materials by means of photoluminescence using micro-Raman apparatus. In: *GeoRaman Xth Meeting*, June 2012, Nancy, France, 11–13.
- BEYSSAC, O., ROUZAUD, J. N., GOFFÉ, B., BRUNET, F. & CHOPIN, C. 2002. Graphitization in a high-pressure, low-temperature metamorphic gradient: a Raman microspectroscopy and HRTEM study. *Contributions to Mineralogy and Petrology*, **143**, 19–31.
- BLATT, H. 1985. Provenance studies and mudrocks. *Journal of Sedimentary Research*, **55**, 69–75.
- BLATT, H. & JONES, R. L. 1975. Proportions of exposed igneous, metamorphic, and sedimentary rocks. *Geological Society of America Bulletin*, **86**, 1085–1088.
- BLATT, H. & SUTHERLAND, B. 1969. Intrastatal solution and non-opaque heavy minerals in mudrocks. *Journal of Sedimentary Petrology*, **39**, 591–600.
- BURGIO, L. & CLARK, R. J. H. 2001. Library of FT-Raman spectra of pigments, minerals, pigment media and varnishes, and supplement to existing library of Raman spectra of pigments with visible excitation. *Spectrochimica Acta, Part A*, **57**, 1491–1521.
- DI PIERRO, S., GNOS, E., GROBETY, B. H., ARMBRUSTER, T., BERNASCONI, S. M. & ULMER, P. 2003. Rock-forming moissanite (natural α -silicon carbide). *American Mineralogist*, **88**, 1817–1821.
- DOWNES, R. T. 2006. The RUFF Project: an integrated study of the chemistry, crystallography, Raman and infrared spectroscopy of minerals. *19th General Meeting of the International Mineralogical Association*, 23–28 July 2006, Kobe, Japan, Program and Abstracts, O03–13.
- FOUCHER, F., LÓPEZ REYES, G., BOST, N., RULL, F., RÜBMAN, P. & WESTALL, F. 2012. Effect of the crushing process on Raman analyses: consequences for the Mars 2018 mission. *Geophysical Research Abstracts*, **14**, EGU2012–4318.
- FREEMAN, J. J., WANG, A., KÜBLER, K. E., JOLLIFF, B. L. & HASKIN, L. A. 2008. Characterization of natural feldspars by Raman spectroscopy for future planetary exploration. *Canadian Mineralogist*, **46**, 1477–1500.
- FREZZOTTI, M. L., SELVERSTONE, J., SHARP, Z. D. & COMPAGNONI, R. 2011. Carbonate dissolution during subduction revealed by diamond-bearing rocks from the Alps. *Nature Geoscience*, **4**, 703–706.
- FREZZOTTI, M. L., TECCE, F. & CASAGLI, A. 2012. Raman spectroscopy for fluid inclusion analysis. *Journal of Geochemical Exploration*, **112**, 1–20.
- GARZANTI, E., ANDÒ, S. & VEZZOLI, G. 2008. Size-density sorting of detrital minerals and grain-size dependence of sediment composition. *Earth Planetary Science Letters*, **273**, 138–151.
- GARZANTI, E., ANDÒ, S., FRANCE-LANORD, C., VEZZOLI, G., GALY, V. & NAJMAN, Y. 2010. Mineralogical and chemical variability of fluvial sediments. 1. Bedload sand (Ganga-Brahmaputra, Bangladesh). *Earth Planetary Science Letters*, **299**, 368–381.
- GARZANTI, E., ANDÒ, S., FRANCE-LANORD, C., CENSI, P., VIGNOLA, P., GALY, V. & LUPKER, M. 2011. Mineralogical and chemical variability of fluvial sediments. 2. Suspended-load silt (Ganga-Brahmaputra, Bangladesh). *Earth Planetary Science Letters*, **302**, 107–120.
- GEIGER, C. A. 2008. Silicate garnet: a micro to macroscopic (re)view. *American Mineralogist*, **93**, 360–372.
- GODOI, R. H. M., POTGIETER-VERMAAK, S., DE HOOG, J., KAEGI, R. & VAN GRIEKEN, R. 2006. Substrate selection for optimum qualitative and quantitative single atmospheric particles analysis using nanomanipulation, sequential thin-window electron probe X-ray microanalysis and micro Raman spectrometry. *Spectrochimica Acta, Part B*, **61**, 375–388.
- GRIFFITH, W. P. 1969. Raman spectroscopy of minerals. *Nature*, **224**, 264–266.
- GUYOT, F., BOYER, H., MADON, M., VELDE, B. & POIRIER, J. P. 1986. Comparison of the Raman microprobe spectra of $(\text{Mg,Fe})_2\text{SiO}_4$ and Mg_2GeO_4 with olivine and spinel structures. *Physics and Chemistry of Minerals*, **13**, 91–95.
- HASKIN, L. A., WANG, A., ROCKOW, K. M., JOLLIFF, B. L., KOROTEV, R. L. & VISKUPIC, K. M. 1997. Raman spectroscopy for mineral identification and quantification for *in situ* planetary surface analysis: a point count method. *Journal of Geophysical Research*, **102**, 19 293–19 306.
- HOPE, G. A., WOODS, R. & MUNCE, C. G. 2001. Raman microprobe mineral identification. *Minerals Engineering*, **14**, 1565–1577.
- KOLESOV, B. A. & GEIGER, C. A. 1998. Raman spectra of silicate garnets. *Physics and Chemistry of Minerals*, **25**, 142–151.
- KÜBLER, K. E., JOLLIFF, B. L., WANG, A. & HASKIN, L. A. 2006. Extracting olivine (Fo–Fa) compositions from Raman spectral peak positions. *Geochimica et Cosmochimica Acta*, **70**, 6201–6222.
- LENZ, C., PETAUTSCHNIG, C., AKHMADALIEV, S., HANF, D., TALLA, D. & NASDALA, L. 2012. Combined Raman and photoluminescence spectroscopic investigation of He-irradiation effects in monazite. *Geophysical Research Abstracts*, **14**, EGU2012–11138.
- MALUSÀ, M. G., CARTER, A., LIMONCELLI, M., GARZANTI, E. & VILLA, I. M. 2013. Bias in detrital zircon geochronology and thermochronometry. *Chemical Geology*, in press.
- MANGE, M. A. & MAURER, H. F. W. 1992. *Heavy Minerals in Colour*. Chapman and Hall, London.
- MANGE, M. A. & WRIGHT, D. T. 2007. High-resolution heavy mineral analysis (HRHMA): a brief summary. In: MANGE, M. A. & WRIGHT, D. T. (eds) *Heavy Minerals in Use*. Elsevier, Amsterdam, Developments in Sedimentology, **58**, 433–436.
- MCMILLAN, P. F. 1989. Raman spectroscopy in mineralogy and geochemistry. *Annual Review of Earth and Planetary Sciences*, **17**, 255–283.
- MERNAGH, T. P. & LIU, L. 1991. Raman spectra from the Al_2SiO_5 polymorphs at high pressure and room temperature. *Physics and Chemistry of Minerals*, **18**, 126–130.
- MORTON, A. C. 1985. Heavy minerals in provenance studies. In: ZUFFA, G. G. (ed.) *Provenance of Arenites*. Reidel, Dordrecht, NATO ASI Series, **148**, 249–277.
- NASDALA, L., PIDGEON, R. T. & WOLF, D. 1996. Heterogeneous metamictization of zircon on microscale. *Geochimica et Cosmochimica Acta*, **60**, 1091–1097.
- NASDALA, L., WENZEL, M., VAVRA, G., IRMER, G., WENZEL, T. & KOBER, B. 2001. Metamictisation of natural zircon: accumulation versus thermal annealing

- of radioactivity-induced damage. *Contributions to Mineralogy and Petrology*, **141**, 125–144.
- NASDALA, L., SMITH, D. C., KAINDL, R. & ZIEMANN, M. 2004. Raman spectroscopy: analytical perspectives in mineralogical research. In: BERAN, A. & LIBOWITZKY, E. (eds) *Spectroscopic Methods in Mineralogy*. Eötvös University Press, Budapest, European Mineralogical Union Notes in Mineralogy, **6**, 281–343.
- NASDALA, L., BEYSSAC, O., SCHOPF, J. W. & BLEIESTEINER, B. 2012. Application of Raman-based images in the Earth Sciences. In: ZOUBIR, A. (ed.) *Raman Imaging*. Springer Series in Optical Sciences, Berlin, **168**, 145–187.
- OSPITALI, F., BERSANI, D., DI LONARDO, G. & LOTTICI, P. P. 2008. 'Green earths': vibrational and elemental characterization of glauconites, celadonites and historical pigments. *Journal of Raman Spectroscopy*, **39**, 1066–1073.
- PALENIK, S. 2007. Heavy minerals in forensic science. In: MANGE, M. A. & WRIGHT, D. T. (eds) *Heavy Minerals in Use*. Elsevier, Amsterdam, Developments in Sedimentology, **58**, 937–961.
- PALMERI, R., FREZZOTTI, M. L., GODARD, G. & DAVIES, R. J. 2009. Pressure-induced incipient amorphization of α -quartz and transition to coesite in an eclogite from Antarctica: a first record and some consequences. *Journal of Metamorphic Geology*, **27**, 685–705.
- POTGIETER-VERMAAK, S. 2007. Surface characterization of a heavy mineral sand with micro-Raman spectrometry. *6th International Heavy Minerals Conference 'Back to Basics'*. The Southern African Institute of Mining and Metallurgy, Johannesburg, 49–53.
- POTGIETER-VERMAAK, S., WOROBIEC, A., DARCHUK, L. & VAN GRIEKEN, R. 2011. Micro-Raman spectroscopy for the analysis of environmental particles. In: SIGNORELLI, R. & REID, J. P. (eds) *Fundamentals and Applications in Aerosol Spectroscopy*. Taylor & Francis, Boca Raton, **8**, 193–208.
- RAMAN, C. V. 1928. A new radiation. *Indian Journal of Physics*, **2**, 387–398.
- SENDOVA, M., ZHELYASKOV, V., SCALERA, M. & RAMSEY, M. 2005. Micro-Raman spectroscopic study of pottery fragments from the Lapatsa Tomb, Cyprus, ca 2500 BC. *Journal of Raman Spectroscopy*, **36**, 829–833.
- SHEBANOVA, O. N. & LAZOR, P. 2003. Raman spectroscopic study of magnetite (FeFe₂O₄): a new assignment for the vibrational spectrum. *Journal of Solid State Chemistry*, **174**, 424–430.
- SILVA, E. N., AYALA, A. P., GUEDES, I., PASCHOAL, C. W. A., MOREIRA, R. L., LOONG, C. K. & BOATNER, L. A. 2006. Vibrational spectra of monazite-type rare-earth orthophosphates. *Optical Materials*, **29**, 224–230.
- SMITH, D. C. 2005. The RAMANITA method for non-destructive and *in situ* semi-quantitative chemical analysis of mineral solid-solutions by multidimensional calibration of Raman wavenumber shifts. *Spectrochimica Acta, Part A*, **61**, 2299–2314.
- STEFANIAK, E. A., WOROBIEC, A., POTGIETER-VERMAAK, S., ALSECCZ, A., TÖRÖK, S. & VAN GRIEKEN, R. 2006. Molecular and elemental characterisation of mineral particles by means of parallel micro-Raman spectrometry and scanning electron microscopy/energy dispersive X-ray analysis. *Spectrochimica Acta, Part B*, **61**, 824–830.
- TOTTEN, M. W. & HANAN, M. A. 2007. Heavy minerals in shales. In: MANGE, M. A. & WRIGHT, D. T. (eds) *Heavy Minerals in Use*. Elsevier, Amsterdam, Developments in Sedimentology Series, **58**, 323–341.
- VANDENABEELE, P., EDWARDS, H. G. M. & MOENS, L. 2007. A decade of Raman spectroscopy in art and archaeology. *Chemical Reviews*, **107**, 675–686.
- VILLANUEVA, U., RAPOSO, J. C., CASTRO, K., DE DIEGO, A., ARANA, G. & MADARIAGA, J. M. 2008. Raman spectroscopy speciation of natural and anthropogenic solid phases in river and estuarine sediments with appreciable amount of clay and organic matter. *Journal of Raman Spectroscopy*, **39**, 1195–1203.
- WANG, A., DHAMELINCOURT, P. & TURRELL, G. 1988. Raman microspectroscopic study of the cation distribution in amphiboles. *Applied Spectroscopy*, **42**, 1441–1450.
- WANG, A., KÜBLER, K. E., JOLLIFF, B. L. & HASKIN, L. A. 2004. Raman spectroscopy of Fe–Ti–Cr-oxides, case study: martian meteorite EETA79001. *American Mineralogist*, **89**, 665–680.
- WANG, A., FREEMAN, J. J., JOLLIFF, B. L. & MING-CHOU, I. 2006. Sulfates on Mars: a systematic Raman spectroscopic study of hydration states of magnesium sulfates. *Geochimica et Cosmochimica Acta*, **70**, 6118–6135.
- WELLS, M. A. & RAMANAIDOU, E. R. 2012. Raman spectroscopic characterisation of Australian banded iron formation and iron ore. *Geophysical Research Abstracts*, **14**, EGU2012–6847.
- WOROBIEC, A., STEFANIAK, E. A., POTGIETER-VERMAAK, S., SAWLOWICZ, Z., SPOLNIK, Z. & VAN GRIEKEN, R. 2007. Characterisation of concentrates of heavy mineral sands by micro-Raman spectrometry and CC-SEM/EDX with HCA. *Applied Geochemistry*, **22**, 2078–2085.
- ZATTIN, M., BERSANI, D. & CARTER, A. 2007. Raman microspectroscopy: a non-destructive tool for routine calibration of apatite crystallographic structure for fission-track analyses. *Chemical Geology*, **240**, 197–204.